2024 European Control Conference (ECC)
June 25-28, 2024. Stockholm, Sweden

Leader-Guided Time-Varying Formation Tracking Control for Multi-Agent Systems under Switching Network Topologies

Ankush Thakur, Tushar Jain

Abstract— **This paper presents a framework designed to address the challenges of runtime formation switching and collision avoidance for multi-agent systems (MASs) operating under undirected and switching network topologies. Within this framework, we investigate time-varying formation tracking (TVFT) control for linear multi-agent systems in the presence of actuator failures and maneuvering leader. One of the main challenges in designing a formation tracking controller is the leader's independent selection of diverse time-varying formation (TVF) configurations for the followers without pre-specifying them, with each configuration lasting for specific durations. To address this challenge, we introduce a set of distributed observers, each concurrently estimating these formation configurations for its assigned follower. Using these estimates and the collision-avoidance algorithm, the proposed controller enables the followers to synchronize with the leader's chosen runtime formations, all without any collisions. Moreover, uniform ultimate boundedness (UUB) of followers' collective formation tracking error is rigorously guaranteed using Lyapunov's stability theory. Finally, a simulation example illustrating the results is given.**

I. Introduction

Formation control for multi-agent systems, a cornerstone of cooperative control, orchestrates group behavior across diverse disciplines like robotics, transportation, control, and communication. This technology continues to revolutionize various fields by enabling functionalities like coordinated robot assembly lines, synchronized drone shows, and distributed communication networks. In most previous research, formation control has been predominantly explored using simplified motion models (i.e., first, second, and high-order integrator dynamics), limiting its applicability to a broad range of practical systems.

TVFT control, as discussed in [1], [2], [3], [10], is an important concept that describes how followers' arrangement (i.e., shape) progresses while tracking the leader. Essentially, TVFT serves as a generalization encompassing consensus, consensus tracking, and formation as its special cases. In the existing literature, researchers investigated TVFT control for both homogeneous [1] and heterogeneous multi-agent systems [2], [3] under various network topologies: undirected [1], directed [2], and switching [3]. However, all prior research [1], [2], [3], [5], [6], [7], [10] has exclusively focused on TVFT control with a predefined follower configuration chosen at the outset. Contrary to existing research, relaxing the scenario (or assumption) of predefined formation opens up possibilities for enhancing the applicability of TVFT, although it would introduce additional complexity into TVFT control. As of our current knowledge, the existing literature has not yet addressed the challenge of TVFT control for non-predefined TVF configurations. In this study, we intend to fill this gap by employing a distributed observer technique.

In practice, due to the phenomenon of link failures and the creation of new links caused by environmental changes, the graph topology may change over time [14], [15]. Thus, studying TVFT control for a non-predefined TVF configuration under switching topologies is practical and significant.

Over the past decade, there has been a notable emphasis on addressing collision avoidance [6], [7], [11], [12] and ensuring fault tolerance [1], [13] in multi-agent systems. In most existing work, the artificial potential field method is the most commonly adopted collision avoidance technique, which depends upon the gradient of the potential function [7], [11], [12] defined for all points in the region of interest, calculated from the sensor field of vision. However, this process needs constant updating of the potential function as the agent maneuvers. To overcome this challenge, we propose an energy-efficient discrete collision avoidance algorithm that eliminates the necessity for continuous updates.

In contrast to studies [1] and [2], which feature simpler analyses due to the leader's control input being zero, resulting in scenarios where the leader either converges to the origin or continuously follows a circular path. However, this work allows the unrestricted maneuvering of the leader by incorporating the methods from [1], [12], which simultaneously adapt to both the leader's maneuvering due to its non-zero control input and actuator faults.

Motivated by the above discussion, the key contributions are listed as follows:

- This paper introduces a novel, distributed observer-based approach for leader-driven runtime formation switching in multi-agent systems (MASs) under switching graph topologies. It departs from prior works where the time-varying formation (TVF) configuration for followers is predetermined. In this approach, followers are unaware of their formation, and the leader solely decides and generates formations in runtime, with the autonomy to maintain the last selection or transition to different ones as needed, all within the scenario of dynamic network connections.
- Here, both the leader's maneuvering and the faults in the followers' actuators are adaptively managed through a single fault-tolerant technique [1].
- This work presents a novel collision avoidance technique that is both discrete and computationally efficient.

Ankush Thakur (d18061@students.iitmandi.ac.in) and Tushar Jain (tushar@iitmandi.ac.in) are with School of Computing and Electrical Engineering, Indian Institute of Technology, Mandi, Himachal Pradesh, India.

II. Preliminaries and Problem formulation

A. Notations and Graph Theory

Let 0_n and 1_n denote column vectors with all n-elements being zeros and ones, respectively. The superscripts $\dagger$ and T represent pseudo matrix inversion and matrix transposition, respectively. Let $\mathbb{Z}_+$ ($\mathbb{Z}_\oplus$), $\mathbb{R}^n$, and $\mathbb{R}^{n\times m}$ represent the sets of positive (non-negative) integers, $(n \times 1)$ real column vectors, and $(n\times m)$ real matrices, respectively. With $y_i \in \mathbb{R}^n$ or $y_i \in \mathbb{R}^{n\times m}$, $i = 1, ..., N$, the vector or matrix $[y_1^{\mathrm{T}}, ..., y_N^{\mathrm{T}}]^{\mathrm{T}}$ is denoted by $\mathrm{col}(y_1, ..., y_N)$. For a given $w \in \mathbb{R}^n$, $\|w\|_j$ represents its j-norm. The notations I_n, $Q \succ \mathbf{0}$, $\lambda_{max}(.)$, $\lambda_{min}(.)$, and $(.\otimes.)$ represent the identity matrix of dimension $(n\times n)$, the positive definite Q, the maximum eigenvalue, the minimum eigenvalue, and the Kronecker product operation, respectively. Let $\mathrm{sig}(z)^b = \mathrm{sign}(z)|z|^b$, where $z \in$ ($\mathbb{R}$ or $\mathbb{R}^n$ or $\mathbb{R}^{n\times m}$), $b > 0$, and $\mathrm{sign}(.)$ is the sign function.

Let the index 0 denote the leader, and the followers are indexed from 1 to N, denoted jointly as $\mathcal{F} = \{1, ..., N\}$. For switching topologies, we consider the set of all possible undirected graphs as $\{\mathscr{G}_{s(t)} : s(t) = 1, ..., M\}$, where $s(t)$ denotes the topology switching signal. In graph $\mathscr{G}_{s(t)}$, the communication links among the followers and between the leader and followers are expressed through the adjacency matrix $\mathcal{A}_{s(t)} = [a_{ij}^{s(t)}] \in \mathbb{R}^{N\times N}$ and the diagonal matrix $\mathrm{diag}(a_{10}^{s(t)}, ..., a_{N0}^{s(t)})$, respectively. The Laplacian matrix of $\mathscr{G}_{s(t)}$ is given as $\mathcal{L}_{s(t)} = [l_{ij}^{s(t)}] \in \mathbb{R}^{N\times N}$ with properties $l_{ii}^{s(t)} = a_{i0}^{s(t)} + \sum_{j=1,j\neq i}^{N} a_{ij}^{s(t)}$ and $l_{ij}^{s(t)} = -a_{ij}^{s(t)}, i \neq j$.

III. Problem statement

A. Agents Dynamics

Consider a multi-agent system with a leader and N followers. The agents' dynamics are as follows:

$$\dot{x}_i(t) = Ax_i(t) + B\big(u_i(t) + f_i(t)\big), \quad i \in \big(\mathcal{F} \cup \{0\}\big), \quad (1)$$

where $x_i(t) \in \mathbb{R}^n$, $u_i(t) \in \mathbb{R}^m$, and $f_i(t) \in \mathbb{R}^m$ are state, control input, and actuator bias fault of i-th agent, respectively. $A \in \mathbb{R}^{n\times n}$ and $B \in \mathbb{R}^{n\times m}$ are known constant matrices. In this work, the leader is assumed to be fault-free, i.e., $f_0(t) = 0_m$.

B. Formation Switching and Key Definitions

The time-varying formation for the followers with respect to the leader as the formation reference is characterized by $h(t) = \mathrm{col}\big(h_1(t), ..., h_N(t)\big) \in \mathbb{R}^{Nn}$. Unlike prior research, this study investigates a scenario where the followers are unaware of $h(t)$, as it is exclusively determined by the leader in runtime, all within the realm of switching topologies.

In this work, suppose the leader has the autonomy to independently select a pair $\Big(C^k, h(t_\alpha^k)\Big)$, $k \in \mathbb{Z}_+$ at $t = t_\alpha^k$, such that $C(t) = C^k$, $\forall\, t \in \big[t_\alpha^k, t_\alpha^{k+1}\big)$ as shown in Fig. 1. Using these selections, the leader determines $h(t)$ for followers from the following switched system [8], [9]:

$$\begin{cases} \dot{h}(t) = \big(I_N \otimes C^k\big)h(t),\; t \in \big[t_\alpha^k, t_\alpha^{k+1}\big), k \in \mathbb{Z}_+, \\ h(t_\alpha^k) = \begin{cases} h_{in}, & \text{if } k = 1; \\ R(k, k-1)\, h(t_\alpha^{k-}) + b(k, k-1), & \text{if } k > 1, \end{cases} \end{cases} \quad (2)$$

where $C^k \in \mathbb{R}^{n\times n}$ represents the formation matrix, and $h_{in} \in \mathbb{R}^{Nn}$ represents the initial formation vector. $R(k, k-1) \in \mathbb{R}^{Nn\times Nn}$ and $b(k, k-1) \in \mathbb{R}^{Nn}$ together define the reset map for adjusting the formation vector at $t = t_\alpha^k$ for $k > 1$.

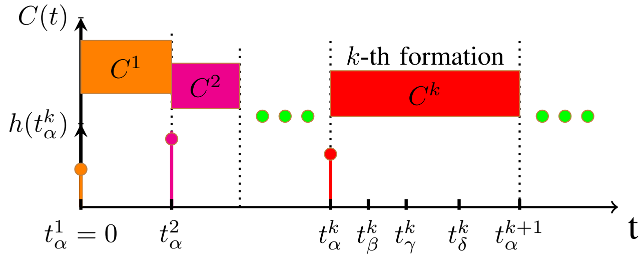

Fig. 1: $\Big\{\big(h(t_\alpha^k), C^k\big)\Big\}_{k\in\mathbb{Z}_+}$ chosen by the leader in runtime.

Furthermore, it's important to mention that the system (1) achieves TVFT for the leader-selected k-th formation, if the following tracking feasibility condition holds:

$$\Big(I_N \otimes (I_n - BB^\dagger)\big(A - C^k\big)\Big)h(t) = 0_{Nn}. \quad (3)$$

Otherwise, TVFT for k-th formation is not achievable.

Here, we introduce significant timestamps that will be frequently mentioned in this paper, defined as follows: Let the time-sequence be $\big\{t_p^k : p \in \{\alpha, \beta, \gamma, \delta\}, k \in \mathbb{Z}_+\big\}$, that satisfies $0 = t_\alpha^1 \leq t_\beta^1 < t_\gamma^1 < t_\delta^1 < t_\alpha^2 \leq t_\beta^2 < t_\gamma^2 < t_\delta^2 < ... < t_\alpha^k \leq t_\beta^k < t_\gamma^k < t_\delta^k < ...$ as shown in Fig. 1, where

- t_α^k is the time stamp at which the leader chooses k-th formation or transitions from $(k-1)$-th to k-th formation.
- t_β^k denotes the time stamp within $\big[t_\alpha^k, t_\alpha^{k+1}\big)$ at which all followers' collective matrix estimation error is zero and remains zero until t_α^{k+1}, i.e., $\widehat{C}(t) - \big(1_N \otimes C^k\big) = 0_{Nn\times n}$, $\forall\, t \in \big[t_\beta^k, t_\alpha^{k+1}\big)$, where $\widehat{C}(t) = \mathrm{col}\big(\widehat{C}^1(t), ..., \widehat{C}^N(t)\big) \in \mathbb{R}^{Nn\times n}$. Here, $\widehat{C}^i(t) \in \mathbb{R}^{n\times n}$, $i \in \mathcal{F}$ is the observer estimate of $C(t)$ for i-th follower.
- t_γ^k denotes the time stamp within $\big[t_\alpha^k, t_\alpha^{k+1}\big)$ at which all followers' collective formation estimation error is zero and remains zero until t_α^{k+1}, i.e., $\widehat{h}(t) - \big(1_N \otimes h(t)\big) = 0_{N^2n}$, $\forall\, t \in \big[t_\gamma^k, t_\alpha^{k+1}\big)$, where $\widehat{h}(t) = \mathrm{col}\big(\widehat{h}^1(t), ..., \widehat{h}^N(t)\big) \in \mathbb{R}^{N^2n}$. Here, $\widehat{h}^i(t) \in \mathbb{R}^{Nn}$, $i \in \mathcal{F}$ is the observer estimate of $h(t)$ for i-th follower.
- t_δ^k denotes the time stamp within $\big[t_\alpha^k, t_\alpha^{k+1}\big)$ at which all followers' collective formation tracking error is ϵ and remains within $\epsilon-$error bound until t_α^{k+1}, i.e., $\big\|x(t) - h(t) - \big(1_N \otimes x_0(t)\big)\big\|_2 \leq \epsilon$, $\forall\, t \in \big[t_\delta^k, t_\alpha^{k+1}\big)$, where $x(t) = \mathrm{col}\big(x_1(t), ..., x_N(t)\big) \in \mathbb{R}^{Nn}$, and $\epsilon > 0$ is the upper bound of the formation tracking error to be evaluated later.

C. Control Objective

The objective is to design methods for collision-avoidance and runtime formation switching in multi-agent systems that operate in undirected and switching topologies. In particular, we aim to achieve collision-free TVFT control for arbitrary formations chosen by the leader in runtime, even under changing graph topologies. Additionally, this work handles challenges due to leader's maneuvering and actuator faults. The followers are said to achieve collision-free TVFT if for any bounded $\{x_i(0)\}_{i=0}^{N}$,

$$\|x_i(t) - h_i(t) - x_0(t)\|_2 \le \epsilon, \forall i \in \mathcal{F}, \quad \forall t \in \big[t_\delta^k, t_\alpha^{k+1}\big), \forall k \in \mathbb{Z}_+$$

holds while ensuring $x_i(t) \neq x_j(t), \forall\, j \in \Big(\big(\{0\} \cup \mathcal{F}\big) \setminus \{i\}\Big)$ for all time under $\mathscr{G}_{s(t)} \in \{\mathscr{G}_1, ..., \mathscr{G}_M\}$.

Furthermore, system (1) adheres to the following assumptions in order to accomplish the above-defined objective.

Assumption 1: The pair (A, B) is stabilizable.

Assumption 2: Each topology graph $\mathscr{G}_{s(t)} \in \{\mathscr{G}_1, ..., \mathscr{G}_M\}$ is connected and remains fixed during $[t_r, t_{r+1})$, where t_r represents the switching instant of $s(t)$, starting at $t_0 = 0$.

Assumption 3: The interval $\big[t_\alpha^k, t_\alpha^{k+1}\big)$ must be of sufficient duration to ensure that the k-th formation can be achieved for all followers.

Assumption 4: The piece-wise constant matrix $C(t)$ is either the zero matrix or possesses simple eigenvalues with real parts equal to zero.

Assumption 5: In (1), $u_0(t)$ and $f_i(t), i \in \mathcal{F}$ are unknown and satisfies $\|u_0(t)\|_2 \le \bar{u}_0$ and $\|f_i(t)\|_2 \le \bar{f}_i$, respectively.

Remark 1: Assumptions 1 and 2 are standard assumptions for controllable and connected MASs [15]. In the absence of assumption 3, a scenario might occur where the leader transitions to the k-th formation without having achieved the $(k-1)$-th formation for all followers. Assumption 4 eliminates impractical formation configurations that exhibit either growing or decaying behavior. Assumption 5 is required for the calculation of ϵ.

IV. Results

A. Design of Formation Observer

The design of adaptive finite-time observer estimating $C(t)$ and $h(t)$ for the i-th follower is constructed as follows:

$$\dot{\widehat{C}}^{i}(t) = -\eta_1 \operatorname{sig}\{H_i^{s(t)}(t)\}^{p_1} - \eta_2 \operatorname{sig}\{H_i^{s(t)}(t)\}^{q_1}, \tag{4a}$$

$$\dot{\widehat{h}}^{i}(t) = \big(I_N \otimes \widehat{C}^{i}(t)\big)\,\widehat{h}^{i}(t) - \wp_i(t)\xi_i^{s(t)}(t) - \eta_3 \operatorname{sig}\{\xi_i^{s(t)}(t)\}^{p_2} - \eta_4 \operatorname{sig}\{\xi_i^{s(t)}(t)\}^{q_2}, \tag{4b}$$

$$\dot{\wp}_i(t) = \big(\xi_i^{s(t)}(t)\big)^T \xi_i^{s(t)}(t), \wp_i(0) = \wp_{i0},\ i \in \mathcal{F}, \tag{4c}$$

where $\widehat{C}^{i}(t) \in \mathbb{R}^{n\times n}$ and $\widehat{h}^{i}(t) = \operatorname{col}\big(\widehat{h_1}^{i}(t), ..., \widehat{h_N}^{i}(t)\big) \in \mathbb{R}^{Nn}$ represent the estimates of $C(t)$ and $h(t)$ for the i-th follower, respectively. Here, $H_i^{s(t)}(t) = \Big(\sum_{j=1}^{N} a_{ij}^{s(t)}\big(\widehat{C}^{i}(t) - \widehat{C}^{j}(t)\big) + a_{i0}^{s(t)}\big(\widehat{C}^{i}(t) - C(t)\big)\Big)$ and $\xi_i^{s(t)}(t) = \Big(\sum_{j=1}^{N} a_{ij}^{s(t)}\big(\widehat{h}^{i}(t) - \widehat{h}^{j}(t)\big) + a_{i0}^{s(t)}\big(\widehat{h}^{i}(t) - h(t)\big)\Big)$. $\wp_i(t)$ is the coupling gain, while p_1, p_2, q_1, q_2, η_1, η_2, η_3, and η_4 are the design parameters satisfying the following Lemma 1.

Lemma 1. Suppose assumptions 2-4 hold, and given that the leader operates system (2). Then, observer achieves

1) For all $k \in \mathbb{Z}_+$, $\lim_{t \to t_\beta^k}\Big(\widehat{C}(t) - \big(1_N \otimes C^k\big)\Big) = 0_{Nn\times n}$ and $\widehat{C}(t) - \big(1_N \otimes C^k\big) = 0_{Nn\times n}$ for all $t \in \big[t_\beta^k, t_\alpha^{k+1}\big)$, if $\eta_1 > 0$, $\eta_2 > 0$, $p_1 > 1$, $q_1 \in (0, 1)$.
2) For all $k \in \mathbb{Z}_+$, $\lim_{t \to t_\gamma^k}\Big(\widehat{h}(t) - \big(1_N \otimes h(t)\big)\Big) = 0_{N^2n}$ and $\widehat{h}(t) - \big(1_N \otimes h(t)\big) = 0_{N^2n}$ for all $t \in \big[t_\gamma^k, t_\alpha^{k+1}\big)$, if $\eta_3 > 0$, $\eta_4 > 0$, $p_2 > 1$, and $q_2 \in (0, 1)$,

where t_β^k and t_γ^k are finite-time settling times. Particularly, $t_\beta^k < t_\beta^{k*}$ and $t_\gamma^k < t_\gamma^{k*}$ with $t_\beta^{k*} = t_\alpha^k + \max_{s(t)\in\{1,...,M\}} \zeta$, $\zeta := \frac{1}{\eta_2(1-q_1)}\Big[\frac{\lambda_{min}(\mathcal{L}_{s(t)}^2)}{\lambda_{max}(\mathcal{L}_{s(t)})}\Big]^{-\frac{1+q_1}{2}} + \frac{n^{p_1} N^{\frac{p_1-1}{2}}}{\eta_1(p_1-1)}\Big[\frac{\lambda_{min}(\mathcal{L}_{s(t)}^2)}{\lambda_{max}(\mathcal{L}_{s(t)})}\Big]^{-\frac{1+p_1}{2}}$.

Proof: The proof will take a similar approach as the one presented in [4], which is not included here.

Remark 2: For all $t \in \big[t_\gamma^k, t_\alpha^{k+1}\big)$, $\forall k \in \mathbb{Z}_+$, achieving $\widehat{h}(t) - \big(1_N \otimes h(t)\big) = 0_{N^2n}$ guarantees $\widehat{h}^{i}(t) = h(t)$ for each follower i $(i \in \mathcal{F})$, and consequently ensures $\widehat{h}_i^{i}(t) = h_i(t)$, which is necessary for the controller to be designed.

B. Collision Avoidance scheme

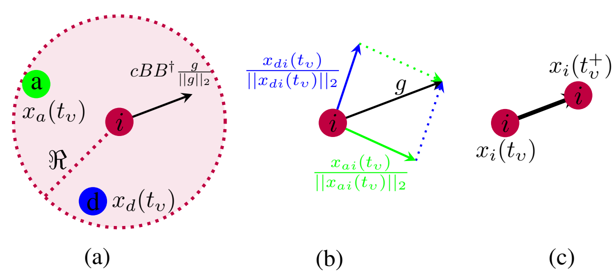

Fig. 3: Collision-avoidance ball $\mathcal{B}\big(x_i(t_\upsilon), \Re\big)$ for i-th follower at $t = t_\upsilon$. Here, $x_{ji}(t_\upsilon) = x_i(t_\upsilon) - x_j(t_\upsilon)$ for $j = a, d$. Additionally, $g := \frac{x_{ai}(t_\upsilon)}{||x_{ai}(t_\upsilon)||_2} + \frac{x_{di}(t_\upsilon)}{||x_{di}(t_\upsilon)||_2}$ and $x_i(t_\upsilon^+) := x_i(t_\upsilon) + cBB^\dagger \frac{g}{||g||_2}$.

Let's define a time sequence $\Delta := \{t_\upsilon : t_\upsilon = \upsilon\Gamma, \upsilon \in \mathbb{Z}_\oplus\}$, where $\Gamma > 0$ is chosen such that no collisions can occur within $[t_\upsilon, t_{\upsilon+1}]$. At each $t = t_\upsilon$, each follower $(i = 1, .., N)$ detects nearby agents within its designated safety zone, known as collision avoidance ball. Specifically, each follower initially identifies agents inside the ball $\mathcal{B}\big(x_i(t_\upsilon), \Re\big)$ at $t = t_\upsilon$, where $x_i(t_\upsilon)$ represents the centre of the ball for the i-th follower, and $\Re$ is its radius. Let $\mathcal{I}_i(t_\upsilon)$ represent the set of agents present inside the collision ball of the follower i at $t = t_\upsilon$, defined as $\mathcal{I}_i(t_\upsilon) := \Big\{j : x_j(t_\upsilon) \in \mathcal{B}\big(x_i(t_\upsilon), \Re\big),\ j \in \big(\{0\} \cup \mathcal{F}\big) \setminus \{i\}\Big\}$. Fig. 3 demonstrates the process: when follower i detects agents a and d within its collision ball at instant $t = t_\upsilon$, then it changes its state impulsively by $cBB^\dagger \frac{g}{||g||_2}$, as shown by the black arrow.

Typically, we employ the superposition principle when two or more agents are detected inside the safety ball of follower i at time instances $t = t_\upsilon \in \mathbb{Z}_{\oplus}$.

Define the collision avoidance component of the control input $u_i(t)$, denoted by $u_i^{ca}(t)$, for each follower as:

$$u_i^{ca}(t) = B^\dagger \sum_{t_\upsilon \in \Delta} \varpi_i(t_\upsilon)\, \text{đ}(t - t_\upsilon), \quad i \in \mathcal{F}, \tag{5}$$

where $\text{đ}(t - t_\upsilon)$ is the unit impulse signal at $t = t_\upsilon$ and

$$\varpi_i(t_\upsilon) = \begin{cases} c\left(\dfrac{\sum_{j\in\mathcal{I}_i(t_\upsilon)}\left(\frac{x_i(t_\upsilon)-x_j(t_\upsilon)}{\|x_i(t_\upsilon)-x_j(t_\upsilon)\|_2}\right)}{\left\|\sum_{j\in\mathcal{I}_i(t_\upsilon)}\left(\frac{x_i(t_\upsilon)-x_j(t_\upsilon)}{\|x_i(t_\upsilon)-x_j(t_\upsilon)\|_2}\right)\right\|_2}\right), & \text{if } \mathcal{I}_i(t_\upsilon) \neq \emptyset; \\ 0_n, & \text{if } \mathcal{I}_i(t_\upsilon) = \emptyset. \end{cases}$$

Here, $c > 0$ is a constant that scales the impulsive shift.

V. Adaptive Controller Design

In addition to $H_i^{s(t)}(t)$ and $\xi_i^{s(t)}(t)$ in (4), each follower requires additional information from its neighborhood, which is described as

$$\begin{aligned} z_i(t) = &\sum_{j=1}^{N} a_{ij}^{s(t)}\Big(\big(x_i(t) - \widehat{h}_i^{\,i}(t)\big) - \big(x_j(t) - \widehat{h}_j^{\,j}(t)\big)\Big) \\ &+ a_{i0}^{s(t)}\big(x_i(t) - \widehat{h}_i^{\,i}(t) - x_0(t)\big), \quad i \in \mathcal{F}, \end{aligned} \tag{6}$$

and writing (6) compactly results in

$$z(t) = (\pounds_{s(t)} \otimes I_n)\Big(x(t) - \widehat{h}^{\star}(t) - \big(1_N \otimes x_0(t)\big)\Big), \tag{7}$$

where $\widehat{h}^{\star}(t) = \text{col}\big(\widehat{h_1}^{1}(t), ..., \widehat{h_N}^{N}(t)\big)$ and $z(t) = \text{col}\big(z_1(t), .., z_N(t)\big)$.

After rearranging (7), we obtain

$$z(t) = (\pounds_{s(t)} \otimes I_n)\big(\varrho(t) - \tilde{h}^{\star}(t)\big), \tag{8}$$

where $\tilde{h}^{\star}(t) = \widehat{h}^{\star}(t) - h(t)$.

In order to synchronize with the leader's chosen runtime formation without any collisions under switching network topologies, the designed adaptive TVFT control protocol, utilizing $\widehat{C}^{\,i}(t)$, $\widehat{h}^{\,i}(t)$, and $z_i(t)$, is proposed as follows:

$$\begin{aligned} u_i(t) &= u_i^{ft}(t) + u_i^{ca}(t) \\ &= \Big\{ -\phi B^{\mathrm{T}}\Xi_{s(t)}\, z_i(t) - \frac{\kappa_i^2(t) B^{\mathrm{T}}\Xi_{s(t)}\, z_i(t)}{\kappa_i(t)\left\|B^{\mathrm{T}}\Xi_{s(t)}\, z_i(t)\right\|_2 + \sigma} \\ &\quad - B^\dagger\big(A - \widehat{C}^{\,i}(t)\big)\widehat{h}_i^{\,i}(t)\Big\} \\ &\quad + \Big\{B^\dagger \sum_{t_\upsilon \in \Delta} \varpi_i(t_\upsilon)\, \text{đ}(t - t_\upsilon)\Big\}, \quad i \in \mathcal{F}, \end{aligned} \tag{9}$$

where $\phi > 0$, $\sigma > 0$, and $\Xi_{s(t)} \succ 0$ are design parameters, $B^\dagger$ is the pseudo inverse of B, and $\kappa_i(t)$ is given as

$$\dot{\kappa_i}(t) = -\varkappa\mu\kappa_i(t) + \varkappa\left\|B^{\mathrm{T}}\Xi_{s(t)}\, z_i(t)\right\|_2, \quad i \in \mathcal{F}, \tag{10}$$

where $\mu > 0$ and $\varkappa > 0$ are design gains.

Let the formation tracking error for the i-th follower be

$$\varrho_i(t) = x_i(t) - h_i(t) - x_o(t), \quad i \in \mathcal{F}. \tag{11}$$

Differentiating (11) and utilizing (9) into the derivative yields

$$\begin{aligned} \dot{\varrho}(t) = &(I_N \otimes A)\,\varrho(t) - \big(I_N \otimes \phi BB^{\mathrm{T}}\Xi_{s(t)}\big)\, z(t) \\ &- \big(I_N \otimes BB^{\mathrm{T}}\Xi_{s(t)}\big)\,\varphi(t) + \vartheta(t) \\ &+ (I_N \otimes B)\Big(f(t) - \big(1_N \otimes u_0(t)\big)\Big) \\ &+ (I_N \otimes BB^\dagger) \sum_{t_\upsilon \in \Delta} \varpi(t_\upsilon)\, \text{đ}(t - t_\upsilon), \end{aligned} \tag{12}$$

where $\varrho(t) = \text{col}\big(\varrho_1(t), ..., \varrho_N(t)\big)$, $f(t) = \text{col}\big(f_1(t), ..., f_N(t)\big)$, $\vartheta_i(t) = \big(A - C(t)\big)h_i(t) - BB^\dagger\big(A - \widehat{C}^{\,i}(t)\big)\widehat{h}_i^{\,i}(t)$, $\vartheta(t) = \text{col}\big(\vartheta_1(t), .., \vartheta_N(t)\big)$, $\varpi(t_\upsilon) = \text{col}\big(\varpi_1(t_\upsilon), .., \varpi_N(t_\upsilon)\big)$, $\varphi(t) = \text{col}\Big(\frac{\kappa_1^2(t) z_1(t)}{\kappa_1(t)\left\|B^{\mathrm{T}}\Xi_{s(t)} z_1(t)\right\|_2 + \sigma}, ..., \frac{\kappa_N^2(t)\, z_N(t)}{\kappa_N(t)\left\|B^{\mathrm{T}}\Xi_{s(t)}\, z_N(t)\right\|_2 + \sigma}\Big)$.

VI. Stability Analysis

Theorem 1: Under all assumptions, consider a MAS satisfying condition (3) with agents (1), where the leader operates another system (2). If, for mode $s(t) = s(t_r)$ during the interval $[t_r, t_{r+1})$, there exists $\Xi_{s(t_r)} \succ \mathbf{0}$ such that

$$\begin{aligned} \Big(A^{\mathrm{T}}\Xi_{s(t_r)} + \Xi_{s(t_r)}A + \varsigma\,\Xi_{s(t_r)} \\ - 2\phi\lambda_{min}(\pounds_{s(t_r)})\,\Xi_{s(t_r)}BB^T\Xi_{s(t_r)}\Big) \prec \mathbf{0}, \end{aligned} \tag{13}$$

then for the followers utilizing observer (4) and controller (9), there exist the time stamps $\{t_\delta^k : k \in \mathbb{Z}_+\}$ such that the TVFT error $\varrho(t)$ is UUB and converges to the

$$\begin{aligned} \Omega := \Big\{\varrho(t) : \|\varrho(t)\|_2 \leq \Big(\frac{1}{\psi}\big(\frac{\theta}{\varsigma} + \rho\big)\Big)^{\frac{1}{2}} =: \epsilon, \\ \forall t \in [t_\delta^k, t_\alpha^{k+1}), \forall k \in \mathbb{Z}_+\Big\}, \end{aligned} \tag{14}$$

where $\varsigma > 0$ and $\rho > 0$ are design parameters. $\theta := 2\sigma N + \mu\sum_{i=1}^{N}\big(\bar{f}_i + \bar{u}_0\big)^2$ and $\psi > 0$ depends on various topologies.

Proof: At time t and mode $s(t) = s(t_r)$ for $t \in [t_r, t_{r+1})$, construct the following topology dependent Lyapunov function as

$$\begin{aligned} V(t) = &\varrho^{\mathrm{T}}(t)\,(\pounds_{s(t_r)} \otimes \Xi_{s(t_r)})\,\varrho(t) \\ &+ \frac{1}{\varkappa}\sum_{i=1}^{N}\Big(\kappa_i(t) - (\bar{f}_i + \bar{u}_0)\Big)^2, \ t \in [t_r, t_{r+1}). \end{aligned} \tag{15}$$

Upon differentiating (15) and subsequently substituting (9) and (10) into the resulting derivative yields

$$\begin{aligned} \dot{V}(t) = &\varrho^{\mathrm{T}}(t)\big(\pounds_{s(t_r)} \otimes (A^{\mathrm{T}}\Xi_{s(t_r)} + \Xi_{s(t_r)}A)\big)\varrho(t) \\ &- \varrho^{\mathrm{T}}(t)\,(\pounds_{s(t_r)} \otimes 2\phi\Xi_{s(t_r)}BB^{\mathrm{T}}\Xi_{s(t_r)})\,z(t) \\ &- 2\varrho^{\mathrm{T}}(t)\,(\pounds_{s(t_r)} \otimes \Xi_{s(t_r)}BB^{\mathrm{T}}\Xi_{s(t_r)})\,\varphi(t) \\ &+ 2\varrho^{\mathrm{T}}(t)\,(\pounds_{s(t_r)} \otimes \Xi_{s(t_r)}BB^\dagger)\sum_{t_\upsilon \in \Delta}\varpi(t_\upsilon)\text{đ}(t - t_\upsilon) \\ &+ 2\varrho^{\mathrm{T}}(t)\,(\pounds_{s(t_r)} \otimes \Xi_{s(t_r)}B)\Big(f(t) - \big(1_N \otimes u_0(t)\big)\Big) \\ &+ 2\varrho^{\mathrm{T}}(t)(\pounds_{s(t_r)} \otimes \Xi_{s(t_r)})\,\vartheta(t) + 2\sum_{i=1}^{N}\Big[\Big(\kappa_i(t) - \big(\bar{f}_i + \bar{u}_0\big)\Big) \\ &\Big(-\mu\kappa_i(t) + \left\|B^{\mathrm{T}}\Xi_{s(t_r)}\, z_i(t)\right\|_2\Big)\Big], \ t \in [t_r, t_{r+1}). \end{aligned} \tag{16}$$

Utilizing (8) in (16) and manipulating subsequently yields

$$\begin{aligned}\dot{V}(t) \leq\ & \varrho^{\mathrm{T}}(t)\Big(\pounds_{s(t_r)} \otimes \big(A^{\mathrm{T}}\Xi_{s(t_r)} + \Xi_{s(t_r)}A \\ & - 2\phi\lambda_{min}(\pounds_{s(t_r)})\Xi_{s(t_r)}BB^{\mathrm{T}}\Xi_{s(t_r)}\big)\Big)\varrho(t) \\ & + \varrho^{\mathrm{T}}(t)\left(\pounds^2_{s(t_r)} \otimes 2\phi\Xi_{s(t_r)}BB^{\mathrm{T}}\Xi_{s(t_r)}\right)\tilde{h}^{\star}(t) \\ & - 2\sum_{i=1}^{N}\frac{\kappa_i^2(t)\left\|B^{\mathrm{T}}\Xi_{s(t_r)}\, z_i(t)\right\|_2^2}{\kappa_i(t)\left\|B^{\mathrm{T}}\Xi_{s(t_r)}\, z_i(t)\right\|_2 + \sigma} \\ & + 2\sum_{i=1}^{N}\kappa_i(t)\left\|B^{\mathrm{T}}\Xi_{s(t_r)}\, z_i(t)\right\|_2 \\ & - 2\big(\tilde{h}^{\star}(t)\big)^{\mathrm{T}}\left(\pounds_{s(t_r)} \otimes \Xi_{s(t_r)}BB^{\mathrm{T}}\Xi_{s(t_r)}\right)\varphi(t) \\ & + 2\varrho^{\mathrm{T}}(t)\left(\pounds_{s(t_r)} \otimes \Xi_{s(t_r)}BB^{\dagger}\right)\sum_{t_\upsilon \in \Delta}\varpi(t_\upsilon)\eth(t-t_\upsilon) \\ & + 2\sum_{i=1}^{N}\left\|B^{\mathrm{T}}\Xi_{s(t_r)}\, z_i(t)\right\|_2\left(\bar{f}_i + \bar{u}_0\right) \\ & + 2\big(\tilde{h}^{\star}(t)\big)^{\mathrm{T}}\left(\pounds_{s(t_r)} \otimes \Xi_{s(t_r)}B\right)\Big(f(t) - \big(1_N \otimes u_0(t)\big)\Big) \\ & + 2\varrho^{\mathrm{T}}(t)\left(\pounds_{s(t_r)} \otimes \Xi_{s(t_r)}\right)\vartheta(t) \\ & - 2\sum_{i=1}^{N}\left(\bar{f}_i + \bar{u}_0\right)\left\|B^{\mathrm{T}}\Xi_{s(t_r)}\, z_i(t)\right\|_2 \\ & - 2\mu\sum_{i=1}^{N}\Big(\kappa_i(t) - \big(\bar{f}_i + \bar{u}_0\big)\Big)\kappa_i(t),\ t \in [t_r, t_{r+1}).\end{aligned} \tag{17}$$

$$\begin{aligned}\dot{V}(t) \leq\ & \varrho^{\mathrm{T}}(t)\Big(\pounds_{s(t_r)} \otimes \big(A^{\mathrm{T}}\Xi_{s(t_r)} + \Xi_{s(t_r)}A \\ & - 2\phi\lambda_{min}(\pounds_{s(t_r)})\Xi_{s(t_r)}BB^{\mathrm{T}}\Xi_{s(t_r)} + \varsigma\Xi_{s(t_r)}\big)\Big)\varrho(t) \\ & - \varsigma V(t) + (\frac{\varsigma}{\varkappa} - \mu)\sum_{i=1}^{N}\Big(\kappa_i(t) - \big(\bar{f}_i + \bar{u}_0\big)\Big)^2 \\ & + \varrho^{\mathrm{T}}(t)\left(\pounds^2_{s(t_r)} \otimes 2\phi\Xi_{s(t_r)}BB^{\mathrm{T}}\Xi_{s(t_r)}\right)\tilde{h}^{\star}(t) + 2\sigma N \\ & - 2\big(\tilde{h}^{\star}(t)\big)^{\mathrm{T}}\left(\pounds_{s(t_r)} \otimes \Xi_{s(t_r)}BB^{\mathrm{T}}\Xi_{s(t_r)}\right)\varphi(t) \\ & + 2\varrho^{\mathrm{T}}(t)\left(\pounds_{s(t_r)} \otimes \Xi_{s(t_r)}BB^{\dagger}\right)\sum_{t_\upsilon \in \Delta}\varpi(t_\upsilon)\eth(t-t_\upsilon) \\ & + 2\big(\tilde{h}^{\star}(t)\big)^{\mathrm{T}}\left(\pounds_{s(t_r)} \otimes \Xi_{s(t_r)}B\right)\Big(f(t) - \big(1_N \otimes u_0(t)\big)\Big) \\ & + \mu\sum_{i=1}^{N}\left(\bar{f}_i + \bar{u}_0\right)^2 + 2\varrho^{\mathrm{T}}(t)\left(\pounds_{s(t_r)} \otimes \Xi_{s(t_r)}\right)\vartheta(t), \\ & t \in [t_r, t_{r+1}).\end{aligned} \tag{18}$$

Using (8), we obtain the following

$$\begin{aligned} & 2\,\varrho^{\mathrm{T}}(t)\left(\pounds_{s(t_r)} \otimes \Xi_{s(t_r)}BB^{\dagger}\right)\sum_{t_\upsilon \in \Delta}\varpi(t_\upsilon)\,\eth(t-t_\upsilon) \\ \leq\ & 2\sum_{t_\upsilon \in \Delta}\Big(\sum_{i=1}^{N}\left\|BB^{\dagger}\Xi_{s(t_r)}\, z_i(t_\upsilon)\right\|_2 \left\|\varpi_i(t_\upsilon)\right\|_2\Big)\eth(t-t_\upsilon) \\ & + 2\sum_{t_\upsilon \in \Delta}\left(\tilde{h}^{\star}(t_\upsilon)\right)^{\mathrm{T}}\left(\pounds_{s(t_r)} \otimes \Xi_{s(t_r)}BB^{\dagger}\right)\varpi(t_\upsilon)\,\eth(t-t_\upsilon).\end{aligned} \tag{19}$$

By selecting $\mu \geq \frac{\varsigma}{\varkappa}$, $\theta := 2\sigma N + \mu\sum_{i=1}^{N}\left(\bar{f}_i + \bar{u}_0\right)^2$, and

$$\Big(A^{\mathrm{T}}\Xi_{s(t_r)} + \Xi_{s(t_r)}A - 2\phi\lambda_{min}(\pounds_{s(t_r)})\Xi_{s(t_r)}BB^{\mathrm{T}}\Xi_{s(t_r)} + \varsigma\Xi_{s(t_r)}\Big) \prec \mathbf{0},$$

in (18), along with the utilization of (19) in (18), we obtain

$$\begin{aligned}\dot{V}(t) \leq\ & -\varsigma V(t) + \theta \\ & + \varrho^{\mathrm{T}}(t)\left(\pounds^2_{s(t_r)} \otimes 2\phi\Xi_{s(t_r)}BB^{\mathrm{T}}\Xi_{s(t_r)}\right)\tilde{h}^{\star}(t) \\ & - 2\big(\tilde{h}^{\star}(t)\big)^{\mathrm{T}}\left(\pounds_{s(t_r)} \otimes \Xi_{s(t_r)}BB^{\mathrm{T}}\Xi_{s(t_r)}\right)\varphi(t) \\ & + 2\sum_{t_\upsilon \in \Delta}\Big(\sum_{i=1}^{N}\left\|BB^{\dagger}\Xi_{s(t_r)}\, z_i(t_\upsilon)\right\|_2 \left\|\varpi_i(t_\upsilon)\right\|_2\Big)\eth(t-t_\upsilon) \\ & + 2\sum_{t_\upsilon \in \Delta}\left(\tilde{h}^{\star}(t_\upsilon)\right)^{\mathrm{T}}\left(\pounds_{s(t_r)} \otimes \Xi_{s(t_r)}BB^{\dagger}\right)\varpi(t_\upsilon)\,\eth(t-t_\upsilon) \\ & + 2\big(\tilde{h}^{\star}(t)\big)^{\mathrm{T}}\left(\pounds_{s(t_r)} \otimes \Xi_{s(t_r)}B\right)\Big(f(t) - \big(1_N \otimes u_0(t)\big)\Big) \\ & + 2\varrho^{\mathrm{T}}(t)(\pounds_{s(t_r)} \otimes \Xi_{s(t_r)})\vartheta(t),\ t \in [t_r, t_{r+1}).\end{aligned} \tag{20}$$

During the k-th formation's interval $\left[t_\alpha^k, t_\alpha^{k+1}\right)$, $k \in \mathbb{Z}_+$, observer (4) estimates $h_i(t)$ as $\widehat{h}_i^{\,i}(t)$ for each follower i over $\left[t_\alpha^k, t_\gamma^k\right)$, and maintains $\widehat{h}_i^{\,i}(t) = h_i(t)$ for the remaining duration $\left[t_\gamma^k, t_\alpha^{k+1}\right)$. Thus, studying system stability during $\left[t_\gamma^k, t_\alpha^{k+1}\right)$ for each $k \in \mathbb{Z}_+$ is crucial.

For $t \in \left[t_\gamma^k, t_\alpha^{k+1}\right)$, $\forall\, k \in \mathbb{Z}_+$, we have $\tilde{h}^{\star}(t) = 0$ and $\vartheta(t) = \Big(I_N \otimes (I_n - BB^{\dagger})\big(A - C(t)\big)\Big)h(t)$ from Lemma 1. Consequently, with (3), $\vartheta(t) = 0$. Thus, (20) reduces to

$$\begin{aligned}\dot{V}(t) \leq\ & -\varsigma V(t) + \theta \\ & + 2\sum_{t_\upsilon \in \Delta}\Big(\sum_{i=1}^{N}\left\|BB^{\dagger}\Xi_{s(t_r)}\, z_i(t_\upsilon)\right\|_2 \left\|\varpi_i(t_\upsilon)\right\|_2\Big)\eth(t-t_\upsilon), \\ & t \in \Big([t_r, t_{r+1}) \cap \left[t_\gamma^k, t_\alpha^{k+1}\right)\Big), k \in \mathbb{Z}_+.\end{aligned} \tag{21}$$

Define $\Lambda^k = \Big([t_r, t_{r+1}) \cap \left[t_\gamma^k, t_\alpha^{k+1}\right)\Big)$. In the subsequent analysis, (21) can take on either of two cases:

Case 1: When $\Lambda^k = \left[t_\gamma^k, t_\alpha^{k+1}\right) \subseteq [t_r, t_{r+1})$, solving (21) for $V(t)$ yields

$$\begin{aligned} V(t) \leq\ & \frac{\theta}{\varsigma} + \Big(V\big(t_\gamma^k\big) - \frac{\theta}{\varsigma}\Big)e^{-\varsigma\left(t - t_\gamma^k\right)} \\ & + 2\sum_{t_\upsilon \in \nabla_\gamma^k}\Big(\Big[\sum_{i=1}^{N}\left\|BB^{\dagger}\Xi_{s(t_r)}\, z_i(t_\upsilon)\right\|_2 \left\|\varpi_i(t_\upsilon)\right\|_2\Big]e^{-\varsigma(t-t_\upsilon)} \\ & \mathfrak{s}(t-t_\upsilon)\Big) \leq \frac{\theta}{\varsigma} + V\big(t_\gamma^k\big)\,e^{-\varsigma\left(t - t_\gamma^k\right)} \\ & + 2\sum_{t_\upsilon \in \nabla_\gamma^k}\Big(\Big[\sum_{i=1}^{N}\left\|BB^{\dagger}\Xi_{s(t_r)}\, z_i(t_\upsilon)\right\|_2 \left\|\varpi_i(t_\upsilon)\right\|_2\Big]e^{-\varsigma(t-t_\upsilon)} \\ & \mathfrak{s}(t-t_\upsilon)\Big), \quad t \in \left[t_\gamma^k, t_\alpha^{k+1}\right),\end{aligned} \tag{22}$$

where $\nabla_\gamma^k := \Big\{t_\upsilon : t_\upsilon = \upsilon\Gamma \geq t_\gamma^k, \upsilon \in \mathbb{Z}_\oplus\Big\}$, and $\mathfrak{s}(t - t_\upsilon)$ is the unit step signal starting at $t = t_\upsilon$.

Case 2: When $\Lambda^k = [t_r, t_{r+1}) \subseteq \big[t_\gamma^k, t_\alpha^{k+1}\big)$ or $[t_r, t_{r+1}) \neq \Lambda^k \neq \big[t_\gamma^k, t_\alpha^{k+1}\big)$, then we define $t_{\gamma,1}^k, ..., t_{\gamma,\mathcal{N}}^k$ as the topology switching instants within $\big[t_\gamma^k, t\big) \subset \big[t_\gamma^k, t_\alpha^{k+1}\big)$, such that $t_\gamma^k =: t_{\gamma,0}^k < t_{\gamma,1}^k < ... < t_{\gamma,\mathcal{N}}^k < t < t_\alpha^{k+1}$.

Combining the solution of (21) under no switching condition with $V\big(t_{\gamma,l}^k\big) \leq \nu V\big(t_{\gamma,l}^{k-}\big)$ for $l = 1, 2, ..., \mathcal{N}$ and applying it iteratively in reverse order, we obtain

$$
\begin{aligned}
V(t) &\leq \frac{\theta}{\varsigma} + \frac{\theta}{\varsigma}\sum_{l=1}^{\mathcal{N}} \nu^l \, e^{-\varsigma\left(t - t_{\gamma,\mathcal{N}-l+1}^k\right)} \\
&+ \nu^{\mathcal{N}} V\big(t_\gamma^k\big) e^{-\varsigma\left(t - t_\gamma^k\right)} + 2\sum_{l=1}^{\mathcal{N}}\Bigg(\nu^{\mathcal{N}-l+1}\Bigg\{\sum_{t_\upsilon \in \nabla_{\gamma,l-1,l}^k} \\
&\Big[\sum_{i=1}^{N}\Big\|BB^\dagger \Xi_{s\left(t_{\gamma,l-1}^k\right)} z_i(t_\upsilon)\Big\|_2 \|\varpi_i(t_\upsilon)\|_2\Big] e^{-\varsigma(t-t_\upsilon)}\mathfrak{s}(t - t_\upsilon) \\
&\Bigg\}\Bigg) + 2\sum_{t_\upsilon \in \nabla_{\gamma,\mathcal{N}}^k}\Bigg(\Big[\sum_{i=1}^{N}\Big\|BB^\dagger \Xi_{s(t_{\gamma,\mathcal{N}}^k)} z_i(t_\upsilon)\Big\|_2 \|\varpi_i(t_\upsilon)\|_2\Big] \\
&e^{-\varsigma(t-t_\upsilon)} \, \mathfrak{s}(t - t_\upsilon)\Bigg), \quad t \in \big[t_{\gamma,\mathcal{N}}^k, t_\alpha^{k+1}\big),
\end{aligned} \tag{23}
$$

where $\nabla_{\gamma,l-1,l}^k = \Big\{t_\upsilon : t_{\gamma,l-1}^k \leq t_\upsilon = \upsilon\Gamma < t_{\gamma,l}^k, \upsilon \in \mathbb{Z}_\oplus\Big\}$ and $\nabla_{\gamma,\mathcal{N}}^k = \Big\{t_\upsilon : t_\upsilon = \upsilon\Gamma \geq t_{\gamma,\mathcal{N}}^k, \upsilon \in \mathbb{Z}_\oplus\Big\}$.

Over time, both (22) and (23) independently transform into (24), as the sum of terms containing decaying exponential terms in (22) and (23) independently can be replaced with ρ such that the following holds:

$$
V(t) \leq \frac{\theta}{\varsigma} + \rho, \quad t \in \big[t_\delta^k, t_\alpha^{k+1}\big). \tag{24}
$$

Define $\psi := \min_{s:=s(t)\in\{1,...,M\}} \{\lambda_{min}(\mathcal{L}_s \otimes \Xi_s)\}$. For $t \in \big[t_\delta^k, t_\alpha^{k+1}\big)$, $k \in \mathbb{Z}_+$, the expression (24) yield $\|\varrho(t)\|_2 \leq \epsilon := \Big(\frac{1}{\psi}\big(\frac{\theta}{\varsigma} + \rho\big)\Big)^{\frac{1}{2}}$, which guarantees $\|\varrho_i(t)\|_2 \leq \epsilon$ for each follower i $(i = 1, ..., N)$ over $\big[t_\delta^k, t_\alpha^{k+1}\big)$. $\square$

VII. Simulation

Agents' Dynamics: $A = \begin{bmatrix} -1 & 1 & 0 \\ 0 & -2 & 0 \\ 0 & 0 & -0.001 \end{bmatrix}$, $B = \begin{bmatrix} 1 & 0 & 0 \\ 1 & 1 & 0 \\ 0 & 0 & 2 \end{bmatrix}$ and $u_0(t) = \begin{cases} 0_3, & t \in [0, 10); \\ \mathrm{col}(-0.1, 0, -0.7), & t \in [10, 20). \end{cases}$

The parameters and faults considered are as follows: $\eta_1 = \eta_2 = \eta_3 = \eta_4 = 5$, $p_1 = p_2 = 1.6$, $q_1 = q_2 = 0.6$, $\phi = 200$, $\sigma = 0.001$, $\varkappa = 600$, $\mu = 0.01$, $\varsigma = 6$, $\Re = 5$, $c = 2.5$, $f_1(t) = \begin{bmatrix} 0.2\cos(t-7) \\ 0 \\ 0.3 \end{bmatrix} \mathfrak{s}(t-7)$, $f_3(t) = \begin{bmatrix} -0.3e^{-0.2(t-7)} \\ 0.5 \\ 0 \end{bmatrix} \mathfrak{s}(t-7)$, $N = 4$, $M = 3$, $-200 \leq u_{i_l}^{ft}(t) \leq 200$ for $i = 1, 2, 3, 4$ and $l = 1, 2, 3$,

Using (13) for $\mathscr{G}_1$: $\Xi_1 = \begin{bmatrix} 0.0987 & -0.0017 & 0 \\ -0.0017 & 0.0225 & 0 \\ 0 & 0 & 0.0327 \end{bmatrix}$.

Similarly, for $\mathscr{G}_2$ and $\mathscr{G}_3$: $\Xi_2 = \begin{bmatrix} 0.0278 & -0.0002 & 0 \\ -0.0002 & 0.0067 & 0 \\ 0 & 0 & 0.01 \end{bmatrix}$ and $\Xi_3 = \begin{bmatrix} 0.0656 & -0.0008 & 0 \\ -0.0008 & 0.0153 & 0 \\ 0 & 0 & 0.0225 \end{bmatrix}$, respectively.

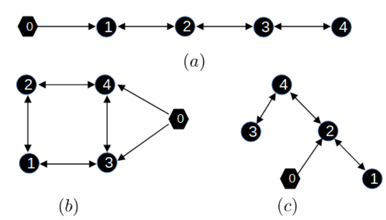

Fig. 4: Interaction graph topologies: (a) $\mathscr{G}_1$; (b) $\mathscr{G}_2$; (c) $\mathscr{G}_3$.

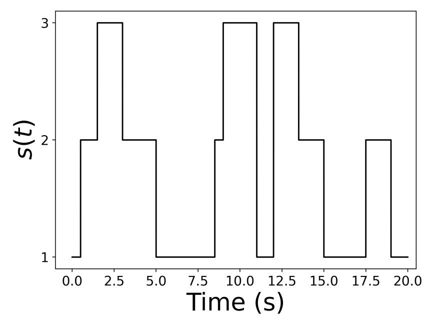

Fig. 5: Switching signal $s(t)$.

To illustrate the leader-guided TVFT control for MAS with the above specifications, consider the scenario where, at $t = t_\alpha^1 = 0$ sec, the leader decides to arrange the followers in the time-invariant V-shape formation. By choosing C^1 and $h(0) = \mathrm{col}\big(h_1(0), ..., h_4(0)\big)$ in (2) at $t = 0$ sec, it generates the time-invariant V-shape formation, where $C^1 = 0_{3\times3}$, $h_1(0) = \begin{bmatrix} 9\cos(45°) \\ 9\sin(45°) \\ 0 \end{bmatrix}$, $h_2(0) = \begin{bmatrix} 9\cos(45°) \\ -9\sin(45°) \\ 0 \end{bmatrix}$, $h_3(0) = \begin{bmatrix} 18\cos(45°) \\ 18\sin(45°) \\ 0 \end{bmatrix}$, and $h_4(0) = \begin{bmatrix} 18\cos(45°) \\ -18\sin(45°) \\ 0 \end{bmatrix}$.

At $t = t_\alpha^2 = 10$ sec, let's assume the leader chooses to transition from the time-invariant V-shape formation to the time-varying circular formation. By choosing $C^2 = \begin{bmatrix} 0 & 2 & 0 \\ -2 & 0 & 0 \\ 0 & 0 & 0 \end{bmatrix}$ and $h(10) = \mathrm{col}\big(h_1(10), ..., h_4(10)\big)$ consisting of $h_i(10) = \begin{bmatrix} 10\cos\big(0.5\pi(i-1)\big) \\ 10\sin\big(0.5\pi(i-1)\big) \\ 0 \end{bmatrix}$, $i = 1, ..., 4$ in (2) at $t = 10$ sec, it generates $h(t) = \mathrm{col}\big(h_1(t), ..., h_4(t)\big)$ consisting of

$$h_i(t)=\begin{bmatrix} 10\cos\left(2t-0.5\pi(i-1)\right) \\ -10\sin\left(2t-0.5\pi(i-1)\right) \\ 0 \end{bmatrix}.$$

The estimate of $h_i(t)$ as $\widehat{h_i}^{\,i}(t)$ for the i-th ($i=1,2,3,4$) follower, obtained using Lemma 1, is depicted in Fig. 6. Fig. 8 contains snapshots showing the alignment of followers in both V-shape and circular formations chosen by the leader. When we view these snapshots in sequence, it illustrates the successful implementation of the proposed leader-guided collision-free TVFT control. Fig. 7 illustrates the convergence of system's TVFT error $\|\varrho(t)\|_2$ to approximate bounded set for both V-shape and circular formations, providing a comprehensive view of the control system's performance. The impact of the pair $\left(f_1(t), f_3(t)\right)$ representing faults and the triplet $\left(u_0(t), f_1(t), f_3(t)\right)$ representing both faults and the leader's control input on $\|\varrho(t)\|_2$ is depicted in the subplot of Fig. 7.

VIII. CONCLUSIONS

In summary, this study presented a novel framework that seamlessly incorporates collision-avoidance and runtime formation switching methods in multi-agent systems operating under switching graph topologies. The follower successfully achieved leader-selected and leader-guided TVFT control utilizing estimates from distributed observers. Notably, the system also demonstrated adaptability by accommodating actuator failures and unrestricted leader maneuvering. This comprehensive approach enhances the robustness and flexibility of MASs, marking a significant advancement in the field of autonomous multi-agent systems.

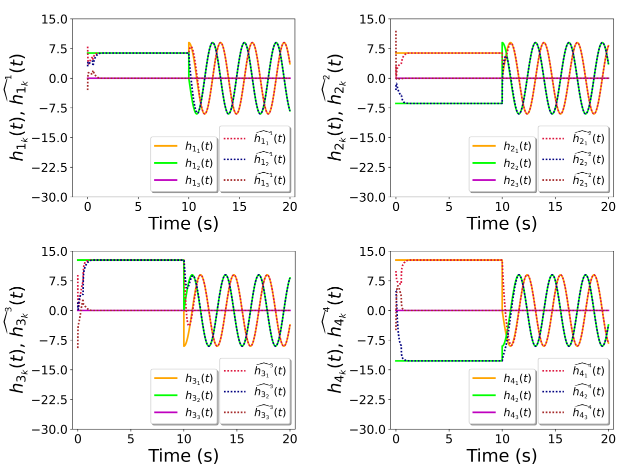

Fig. 6: Estimation of $h_i(t)$ for follower i ($i=1,2,3,4$).

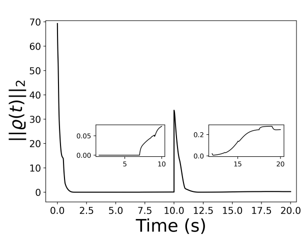

Fig. 7: TVFT error norm $\|\varrho(t)\|_2$.

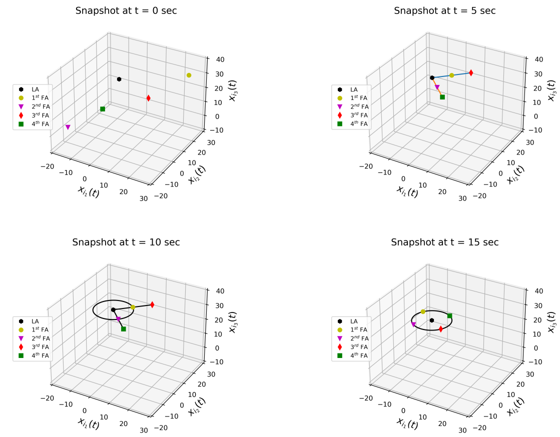

Fig. 8: Compilation of state snapshots.

REFERENCES

[1] Liu, Fei, et al. "Adaptive fault-tolerant time-varying formation tracking for multi-agent systems under actuator failure and input saturation." ISA transactions 104 (2020): 145-153.

[2] Hua, Yongzhao, et al. "Time-varying output formation tracking of heterogeneous linear multi-agent systems with multiple leaders and switching topologies." Journal of the Franklin Institute 356.1 (2019): 539-560.

[3] Liu, Congying, et al. "Time-varying output formation tracking of heterogeneous linear multi-agent systems with dynamical controllers." Neurocomputing 441 (2021): 36-43.

[4] Zhang, Huaguang, et al. "Bipartite fixed-time output consensus of heterogeneous linear multiagent systems." IEEE transactions on cybernetics 51.2 (2019): 548-557.

[5] Li, Weixun, Zengqiang Chen, and Zhongxin Liu. "Leader-following formation control for second-order multiagent systems with time-varying delay and nonlinear dynamics." Nonlinear Dynamics 72 (2013): 803-812.

[6] Liu, Yutong, et al. "Formation control and collision avoidance for a class of multi-agent systems." Journal of the Franklin Institute 356.10 (2019): 5395-5420.

[7] Shi, Quan, et al. "Adaptive leader-following formation control with collision avoidance for a class of second-order nonlinear multi-agent systems." Neurocomputing 350 (2019): 282-290.

[8] Jiao, Ticao, Wei Xing Zheng, and Shengyuan Xu. "Unified stability criteria of random nonlinear time-varying impulsive switched systems." IEEE Transactions on Circuits and Systems I: Regular Papers 67.9 (2020): 3099-3112.

[9] Thakur, Ankush, and Tushar Jain. "Practical Time-Varying Formation Tracking Control for Multi-Agent Systems." 2023 American Control Conference (ACC). IEEE, 2023.

[10] Han, Liang, et al. "Time-varying group formation tracking control for second-order multi-agent systems with communication delays and multiple leaders." Journal of the Franklin Institute 357.14 (2020): 9761-9780.

[11] Li, Qi, et al. "Distributed adaptive fixed-time formation control for second-order multi-agent systems with collision avoidance." Information Sciences 564 (2021): 27-44.

[12] Hwang, Jiyoon, Jinah Lee, and Chandeok Park. "Collision avoidance control for formation flying of multiple spacecraft using artificial potential field." Advances in Space Research 69.5 (2022): 2197-2209.

[13] Hua, Yongzhao, et al. "Distributed fault-tolerant time-varying formation control for high-order linear multi-agent systems with actuator failures." ISA transactions 71 (2017): 40-50.

[14] Deng, Chao, and Wei-Wei Che. "Fault-tolerant fuzzy formation control for a class of nonlinear multiagent systems under directed and switching topology." IEEE Transactions on Systems, Man, and Cybernetics: Systems 51.9 (2019): 5456-5465.

[15] Zhang, Shuo, et al. "Topology-based dynamic event-triggered leader-following consensus of multi-agent systems under switching topologies." ISA transactions (2023).